



HAL
open science

A measurement of A^b_{FB} in lifetime tagged heavy flavour Z decays

D. Buskulic, D. Casper, I. de Bonis, D. Decamp, P. Ghez, C. Goy, J P. Lees,
M N. Minard, P. Odier, B. Pietrzyk, et al.

► **To cite this version:**

D. Buskulic, D. Casper, I. de Bonis, D. Decamp, P. Ghez, et al.. A measurement of A^b_{FB} in lifetime tagged heavy flavour Z decays. Physics Letters B, 1994, 335, pp.99-108. in2p3-00004334

HAL Id: in2p3-00004334

<https://in2p3.hal.science/in2p3-00004334v1>

Submitted on 27 Mar 2000

HAL is a multi-disciplinary open access archive for the deposit and dissemination of scientific research documents, whether they are published or not. The documents may come from teaching and research institutions in France or abroad, or from public or private research centers.

L'archive ouverte pluridisciplinaire **HAL**, est destinée au dépôt et à la diffusion de documents scientifiques de niveau recherche, publiés ou non, émanant des établissements d'enseignement et de recherche français ou étrangers, des laboratoires publics ou privés.

A Measurement of A_{FB}^b in Lifetime Tagged Heavy Flavour Z Decays

The ALEPH Collaboration

Abstract

A new measurement of the forward-backward asymmetry in $Z \rightarrow b\bar{b}$ decays is presented. Hadrons from b decays are tagged using their long lifetimes. The b quark charge and direction are reconstructed with a hemisphere charge algorithm. The asymmetry and reconstructed b hemisphere charge are measured in the 69 pb^{-1} of data collected by ALEPH during 1991, 1992 and 1993. They are used to extract $\sin^2\theta_W^{eff}$, which is determined to be $0.2315 \pm 0.0016(stat.) \pm 0.0009(syst.)$, corresponding to an A_{FB}^b of $0.0992 \pm 0.0084(stat.) \pm 0.0046(syst.)$.

(Submitted to Physics Letters B)

The ALEPH Collaboration

D. Buskulic, D. Casper, I. De Bonis, D. Decamp, P. Ghez, C. Goy, J.-P. Lees, M.-N. Minard, P. Odier, B. Pietrzyk

Laboratoire de Physique des Particules (LAPP), IN²P³-CNRS, 74019 Annecy-le-Vieux Cedex, France

F. Ariztizabal, M. Chmeissani, J.M. Crespo, I. Efthymiopoulos, E. Fernandez, M. Fernandez-Bosman, V. Gaitan, Ll. Garrido,²⁸ M. Martinez, T. Mattison,²⁹ S. Orteu, A. Pacheco, C. Padilla, F. Palla, A. Pascual, J.A. Perlas, F. Teubert

Institut de Fisica d'Altes Energies, Universitat Autònoma de Barcelona, 08193 Bellaterra (Barcelona), Spain⁷

D. Creanza, M. de Palma, A. Farilla, G. Iaselli, G. Maggi, N. Marinelli, S. Natali, S. Nuzzo, A. Ranieri, G. Raso, F. Romano, F. Ruggieri, G. Selvaggi, L. Silvestris, P. Tempesta, G. Zito

Dipartimento di Fisica, INFN Sezione di Bari, 70126 Bari, Italy

Y. Chai, D. Huang, X. Huang, J. Lin, T. Wang, Y. Xie, D. Xu, R. Xu, J. Zhang, L. Zhang, W. Zhao

Institute of High-Energy Physics, Academia Sinica, Beijing, The People's Republic of China⁸

G. Bonvicini, J. Boudreau,²⁵ P. Comas, P. Coyle, H. Drevermann, A. Engelhardt, R.W. Forty, G. Ganis, C. Gay,³ M. Girone, R. Hagelberg, J. Harvey, R. Jacobsen, B. Jost, J. Knobloch, I. Lehraus, M. Maggi, C. Markou, P. Mato, H. Meinhard, A. Minten, R. Miquel, P. Palazzi, J.R. Pater, P. Perrodo, J.-F. Pustaszari, F. Ranjard, L. Rolandi, J. Rothberg,² M. Saich,⁶ D. Schlatter, M. Schmelling, W. Tejessy, I.R. Tomalin, R. Veenhof, A. Venturi, H. Wachsmuth, S. Wasserbaech,² W. Wiedenmann, T. Wildish, W. Witzeling, J. Wotschack

European Laboratory for Particle Physics (CERN), 1211 Geneva 23, Switzerland

Z. Ajaltouni, M. Bardadin-Otwinowska, A. Barres, C. Boyer, A. Falvard, P. Gay, C. Guicheney, P. Henrard, J. Jousset, B. Michel, J-C. Montret, D. Pallin, P. Perret, F. Podlyski, J. Proriot, F. Saadi

Laboratoire de Physique Corpusculaire, Université Blaise Pascal, IN²P³-CNRS, Clermont-Ferrand, 63177 Aubière, France

T. Fearnley, J.B. Hansen, J.D. Hansen, J.R. Hansen, P.H. Hansen, S.D. Johnson, R. Møllerud, B.S. Nilsson

Niels Bohr Institute, 2100 Copenhagen, Denmark⁹

A. Kyriakis, E. Simopoulou, I. Siotis, A. Vayaki, K. Zachariadou

Nuclear Research Center Demokritos (NRCD), Athens, Greece

A. Blondel, G. Bonneaud, J.C. Brient, P. Bourdon, L. Passalacqua, A. Rougé, M. Rumpf, R. Tanaka, A. Valassi, M. Verderi, H. Videau

Laboratoire de Physique Nucléaire et des Hautes Energies, Ecole Polytechnique, IN²P³-CNRS, 91128 Palaiseau Cedex, France

D.J. Candlin, M.I. Parsons, E. Veitch

Department of Physics, University of Edinburgh, Edinburgh EH9 3JZ, United Kingdom¹⁰

E. Focardi, G. Parrini

Dipartimento di Fisica, Università di Firenze, INFN Sezione di Firenze, 50125 Firenze, Italy

M. Corden, M. Delfino,¹² C. Georgiopoulos, D.E. Jaffe, D. Levinthal¹⁵

Supercomputer Computations Research Institute, Florida State University, Tallahassee, FL 32306-4052, USA^{13,14}

A. Antonelli, G. Bencivenni, G. Bologna,⁴ F. Bossi, P. Campana, G. Capon, F. Cerutti, V. Chiarella, G. Felici, P. Laurelli, G. Mannocchi,⁵ F. Murtas, G.P. Murtas, M. Pepe-Altarelli, S. Salomone

Laboratori Nazionali dell'INFN (LNF-INFN), 00044 Frascati, Italy

P. Colrain, I. ten Have, I.G. Knowles, J.G. Lynch, W. Maitland, W.T. Morton, C. Raine, P. Reeves, J.M. Scarr, K. Smith, M.G. Smith, A.S. Thompson, S. Thorn, R.M. Turnbull

Department of Physics and Astronomy, University of Glasgow, Glasgow G12 8QQ, United Kingdom¹⁰

U. Becker, O. Braun, C. Geweniger, P. Hanke, V. Hepp, E.E. Kluge, A. Putzer,¹ B. Rensch, M. Schmidt, H. Stenzel, K. Tittel, M. Wunsch

Institut für Hochenergiephysik, Universität Heidelberg, 69120 Heidelberg, Fed. Rep. of Germany¹⁶

R. Beuselinck, D.M. Binnie, W. Cameron, M. Cattaneo, D.J. Colling, P.J. Dornan, J.F. Hassard, N. Konstantinidis, L. Moneta, A. Moutoussi, J. Nash, D.G. Payne, G. San Martin, J.K. Sedgbeer, A.G. Wright

Department of Physics, Imperial College, London SW7 2BZ, United Kingdom¹⁰

P. Girtler, D. Kuhn, G. Rudolph, R. Vogl

Institut für Experimentalphysik, Universität Innsbruck, 6020 Innsbruck, Austria¹⁸

C.K. Bowdery, T.J. Brodbeck, A.J. Finch, F. Foster, G. Hughes, D. Jackson, N.R. Keemer, M. Nuttall, A. Patel, T. Sloan, S.W. Snow, E.P. Whelan

Department of Physics, University of Lancaster, Lancaster LA1 4YB, United Kingdom¹⁰

A. Galla, A.M. Greene, K. Kleinknecht, J. Raab, B. Renk, H.-G. Sander, H. Schmidt, S.M. Walther, R. Wanke, B. Wolf

Institut für Physik, Universität Mainz, 55099 Mainz, Fed. Rep. of Germany¹⁶

A.M. Bencheikh, C. Benchouk, A. Bonissent, D. Calvet, J. Carr, C. Diaconu, F. Etienne, D. Nicod, P. Payre, L. Roos, D. Rousseau, P. Schwemling, M. Talby

Centre de Physique des Particules, Faculté des Sciences de Luminy, IN²P³-CNRS, 13288 Marseille, France

S. Adlung, R. Assmann, C. Bauer, W. Blum, D. Brown, P. Cattaneo,²³ B. Dehning, H. Dietl, F. Dydak,²¹ M. Frank, A.W. Halley, K. Jakobs, H. Kroha, J. Lauber, G. Lütjens, G. Lutz, W. Männer, H.-G. Moser, R. Richter, S. Schael, J. Schröder, A.S. Schwarz, R. Settles, H. Seywerd, U. Stierlin,³⁰ U. Stiegler, R. St. Denis, G. Wolf

Max-Planck-Institut für Physik, Werner-Heisenberg-Institut, 80805 München, Fed. Rep. of Germany¹⁶

R. Alemany, J. Boucrot, O. Callot, A. Cordier, F. Courault, M. Davier, L. Duflot, J.-F. Grivaz, Ph. Heusse, P. Janot, M. Jacquet, D.W. Kim,¹⁹ F. Le Diberder, J. Lefrançois, A.-M. Lutz, G. Musolino, I. Nikolic, H.J. Park, I.C. Park, S. Simion, M.-H. Schune, J.-J. Veillet, I. Videau

Laboratoire de l'Accélérateur Linéaire, Université de Paris-Sud, IN²P³-CNRS, 91405 Orsay Cedex, France

D. Abbaneo, G. Bagliesi, G. Batignani, U. Bottigli, C. Bozzi, G. Calderini, M. Carpinelli, M.A. Ciocci, V. Ciulli, R. Dell'Orso, I. Ferrante, F. Fidecaro, L. Foà,¹ F. Forti, A. Giassi, M.A. Giorgi, A. Gregorio, F. Ligabue, A. Lusiani, P.S. Marrocchesi, E.B. Martin, A. Messineo, G. Rizzo, G. Sanguinetti, P. Spagnolo, J. Steinberger, R. Tenchini,¹ G. Tonelli,²⁷ G. Triggiani, C. Vannini, P.G. Verdini, J. Walsh

Dipartimento di Fisica dell'Università, INFN Sezione di Pisa, e Scuola Normale Superiore, 56010 Pisa, Italy

A.P. Betteridge, Y. Gao, M.G. Green, D.L. Johnson, P.V. March, T. Medcalf, L.I.M. Mir, I.S. Quazi, J.A. Strong

Department of Physics, Royal Holloway & Bedford New College, University of London, Surrey TW20 OEX, United Kingdom¹⁰

V. Bertin, D.R. Botterill, R.W. Clift, T.R. Edgecock, S. Haywood, M. Edwards, P.R. Norton, J.C. Thompson

Particle Physics Dept., Rutherford Appleton Laboratory, Chilton, Didcot, Oxon OX11 0QX, United Kingdom¹⁰

B. Bloch-Devaux, P. Colas, H. Duarte, S. Emery, W. Kozanecki, E. Lançon, M.C. Lemaire, E. Locci, B. Marx, P. Perez, J. Rander, J.-F. Renardy, A. Rosowsky, A. Roussarie, J.-P. Schuller, J. Schwindling, D. Si Mohand, B. Vallage

*CEA, DAPNIA/Service de Physique des Particules, CE-Saclay, 91191 Gif-sur-Yvette Cedex, France*¹⁷

R.P. Johnson, A.M. Litke, G. Taylor, J. Wear

*Institute for Particle Physics, University of California at Santa Cruz, Santa Cruz, CA 95064, USA*²²

A. Beddall, C.N. Booth, S. Cartwright, F. Combley, I. Dawson, A. Koksal, C. Rankin, L.F. Thompson
*Department of Physics, University of Sheffield, Sheffield S3 7RH, United Kingdom*¹⁰

A. Böhrrer, S. Brandt, G. Cowan,¹ E. Feigl, C. Grupen, G. Lutters, J. Minguet-Rodriguez, F. Rivera,²⁶
P. Saraiva, U. Schäfer, L. Smolik

*Fachbereich Physik, Universität Siegen, 57068 Siegen, Fed. Rep. of Germany*¹⁶

L. Bosisio, R. Della Marina, G. Giannini, B. Gobbo, L. Pitis, F. Ragusa²⁰

Dipartimento di Fisica, Università di Trieste e INFN Sezione di Trieste, 34127 Trieste, Italy

L. Bellantoni, J.S. Conway,²⁴ Z. Feng, D.P.S. Ferguson, Y.S. Gao, J. Grahl, J.L. Harton, O.J. Hayes, H. Hu, J.M. Nachtman, Y.B. Pan, Y. Saadi, M. Schmitt, I. Scott, V. Sharma, J.D. Turk, A.M. Walsh, F.V. Weber,¹ Sau Lan Wu, X. Wu, J.M. Yamartino, M. Zheng, G. Zobernig

*Department of Physics, University of Wisconsin, Madison, WI 53706, USA*¹¹

¹Now at CERN, PPE Division, 1211 Geneva 23, Switzerland.

²Permanent address: University of Washington, Seattle, WA 98195, USA.

³Now at Harvard University, Cambridge, MA 02138, U.S.A.

⁴Also Istituto di Fisica Generale, Università di Torino, Torino, Italy.

⁵Also Istituto di Cosmo-Geofisica del C.N.R., Torino, Italy.

⁶Now at Parallax, UK.

⁷Supported by CICYT, Spain.

⁸Supported by the National Science Foundation of China.

⁹Supported by the Danish Natural Science Research Council.

¹⁰Supported by the UK Science and Engineering Research Council.

¹¹Supported by the US Department of Energy, contract DE-AC02-76ER00881.

¹²On leave from Universitat Autònoma de Barcelona, Barcelona, Spain.

¹³Supported by the US Department of Energy, contract DE-FG05-92ER40742.

¹⁴Supported by the US Department of Energy, contract DE-FC05-85ER250000.

¹⁵Present address: Lion Valley Vineyards, Cornelius, Oregon, U.S.A.

¹⁶Supported by the Bundesministerium für Forschung und Technologie, Fed. Rep. of Germany.

¹⁷Supported by the Direction des Sciences de la Matière, C.E.A.

¹⁸Supported by Fonds zur Förderung der wissenschaftlichen Forschung, Austria.

¹⁹Permanent address: Kangnung National University, Kangnung, Korea.

²⁰Now at Dipartimento di Fisica, Università di Milano, Milano, Italy.

²¹Also at CERN, PPE Division, 1211 Geneva 23, Switzerland.

²²Supported by the US Department of Energy, grant DE-FG03-92ER40689.

²³Now at Università di Pavia, Pavia, Italy.

²⁴Now at Rutgers University, Piscataway, NJ 08854, USA.

²⁵Now at University of Pittsburgh, Pittsburgh, PA 15260, U.S.A.

²⁶Partially supported by Colciencias, Colombia.

²⁷Also at Istituto di Matematica e Fisica, Università di Sassari, Sassari, Italy.

²⁸Permanent address: Dept. d'Estructura i Constituents de la Matèria, Universitat de Barcelona, 08208 Barcelona, Spain.

²⁹Now at SLAC, Stanford, CA 94309, U.S.A.

³⁰Deceased.

1 Introduction

As the volume of recorded LEP data grows, it is of interest to study how new measurements of Z decays to specific quark flavours can afford added sensitivity to electroweak parameters. One example is the forward-backward asymmetry of quark-antiquark (or $f\bar{f}$) production. The asymmetry is defined using the angle, θ , between the incoming electron and the outgoing fermion to denote the forward ($\cos\theta > 0$) and backward ($\cos\theta < 0$) hemispheres :

$$A_{FB}^f = \frac{\sigma_F^f - \sigma_B^f}{\sigma_F^f + \sigma_B^f}$$

To relate A_{FB}^f to Standard Model Z couplings, corrections must be made for detector effects and for QED and QCD radiation. At the parton level, the latter are -4% and -2.7% respectively [1, 2] for the case of the b quark. Applying these corrections allows the effective weak mixing angle, $\sin^2\theta_W^{eff}$, to be extracted. The sensitivity of A_{FB}^f to $\sin^2\theta_W^{eff}$ is greater than that of lepton asymmetries and is compounded with the rates of quark production which are significantly greater than the total rate of Z decays to leptons.

An asymmetry measurement needs to distinguish quarks from antiquarks and it is useful to separate the Z decays into up and down-type quarks. The latter avoids cancellation between quark flavours. Experimentally, both these criteria are currently practicable only for heavy flavour decays. This is especially true in the case of the b quark which has a large production rate, mass and lifetime.

Heavy flavour tagging has been performed previously using the presence of a lepton from semileptonic decays, where the lepton charge is used to sign the direction of the parent quark [3, 4]. More recently silicon strip tracking detectors have been used to select heavy flavours as a result of their long lifetimes, leading to unprecedented purities and tagging efficiencies [5]. This is the approach employed here. A disadvantage of such a lifetime tag is that the charges of the quark and antiquark are not directly observed. They are reconstructed on a statistical basis from fragmentation and decay products using the hemisphere charge technique described in [6]. This tempers somewhat the increased statistical power afforded by the lifetime tag and results in a new measurement with a similar precision to that of semileptonic measurements.

2 Principles of the Method

A measurement of the charge asymmetry in an enriched heavy flavour sample is used to study the asymmetry of the b quark, A_{FB}^b . Each event is divided into hemispheres by a plane perpendicular to the thrust axis, \vec{T} , which is orientated to point in the forward direction. Hemisphere charges are formed using a summation over particle charges, q , weighted by their momentum, \vec{p} :

$$Q_F = \frac{\sum_i^{\vec{p}_i \cdot \vec{T} > 0} |\vec{p}_i \cdot \vec{T}|^\kappa q_i}{\sum_i^{\vec{p}_i \cdot \vec{T} > 0} |\vec{p}_i \cdot \vec{T}|^\kappa} \quad (1)$$

and analogously for Q_B . The κ parameter is used to optimise the measurement sensitivity. A quark asymmetry is then proportional to the mean charge flow, $\langle Q_{FB}^f \rangle$, between forward and backward hemispheres :

$$\langle Q_{FB}^f \rangle = \langle Q_F - Q_B \rangle = \delta_f A_{FB}^f$$

δ_f is defined as the charge separation for a quark of flavour f . The total charge, $\langle Q^f \rangle$, is given by $\langle Q_F + Q_B \rangle$ and remains close to zero.

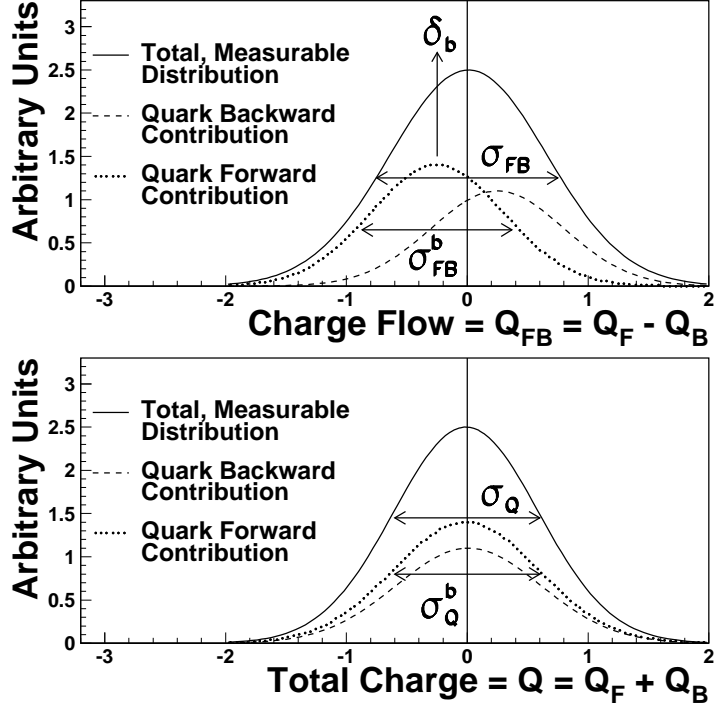


Figure 1: Illustration of the Q_{FB} and Q charge distributions for b quarks. σ_{FB}^b and σ_Q^b are the widths of the Q_{FB} and Q distributions for the cases when the b quark went forward.

The same sample of events used to measure $\langle Q_{FB} \rangle$ can be used to extract δ_f . A single hemisphere charge measurement, Q_f , may be written as :

$$Q_f = \frac{\delta_f}{2} + \mathcal{R}_f \quad \text{and} \quad Q_{\bar{f}} = \frac{\delta_{\bar{f}}}{2} + \mathcal{R}_{\bar{f}}$$

where \mathcal{R} is the measurement error due to fragmentation and detector effects. The product of the two hemisphere charges then averages to :

$$\langle Q_f Q_{\bar{f}} \rangle = \langle Q_F Q_B \rangle = \frac{-\delta_f^2}{4} + \langle \mathcal{R}_f \mathcal{R}_{\bar{f}} \rangle$$

using $\delta_f = -\delta_{\bar{f}}$ and assuming that $\mathcal{R}_f - \mathcal{R}_{\bar{f}}$ averages to zero. The measurement error correlation, $\langle \mathcal{R}_f \mathcal{R}_{\bar{f}} \rangle$, arises from sharing a common axis and crossover of particles close to the hemisphere boundary. It is small and insensitive to the details of fragmentation. In practice, $\langle Q_F Q_B \rangle$ is measured from the difference in variances, σ_{FB} and σ_Q , of the Q_{FB} and Q distributions respectively. This is illustrated in Figure 1. It is then useful to define :

$$\begin{aligned} \bar{\delta}_f^2 &= \left(\sigma_{FB}^f \right)^2 - \left(\sigma_Q^f \right)^2 = -4 \langle Q_F Q_B \rangle - \langle Q_{FB}^f \rangle^2 + \langle Q^f \rangle^2 \\ &= \delta_f^2 - 4 \langle \mathcal{R}_f \mathcal{R}_{\bar{f}} \rangle - \langle Q_{FB}^f \rangle^2 + \langle Q^f \rangle^2 \end{aligned} \quad (2)$$

The quantities, $\bar{\delta}$, $\langle Q_{FB} \rangle$ and $\langle Q \rangle$ are measured directly in a data sample enriched with heavy flavours. The enrichment results from selecting events possessing several particles with significant impact parameters. The impact parameter of a charged particle is defined as the distance of closest approach of its linearised track to the interaction point. The track helix is linearised at its point of closest approach to the estimated b hadron flight direction, approximated by a reconstructed jet. The impact parameter is signed positive if the point of closest approach

to the jet lies on the same side of the primary interaction point as the jet direction, and negative otherwise. Negative impact parameter tracks are used to estimate the resolution in data while the significance of positive impact parameter particles are used to calculate the probability that the hemisphere arises from u, d, s quark production. Events are selected as having hemispheres with probabilities less than a given cut. Reducing the cut increases the heavy flavour composition of the tagged sample [5].

Denoting the flavour composition of the sample by the purities $(\mathcal{P}_u, \mathcal{P}_d, \mathcal{P}_s, \mathcal{P}_c, \mathcal{P}_b)$, where $\mathcal{P}_b \gg \mathcal{P}_{u,d,s,c}$, then A_{FB}^b may be written as :

$$A_{FB}^b = \frac{1}{\mathcal{P}_b C_b} \left[\frac{\langle Q_{FB} \rangle}{\delta_b} - \frac{1}{\delta_b} \sum_{f=u,d,\dots}^c \mathcal{P}_f C_f \delta_f A_{FB}^f \right] \quad (3)$$

where C_f are flavour dependent acceptance factors. Both $\langle Q_{FB} \rangle$ and δ_b measurements are needed to extract A_{FB}^b .

The charge separation, δ_b , is defined with respect to the original $b\bar{b}$ pair orientation, prior to $B^0\bar{B}^0$ mixing and gluon radiation. It is of interest to note that the above method of extracting δ_b from $\bar{\delta}$ in data naturally incorporates the dilution of the b hemisphere charge from these effects. Hence, in contrast to semileptonic measurements, no such correction or uncertainty need be applied to the measured asymmetry.

3 The ALEPH Detector

The ALEPH detector is described in detail elsewhere [7] and only those features relevant for the current analysis are given here. The tracking is based on a time-projection chamber (TPC) in conjunction with an inner tracking chamber (ITC) and silicon vertex detector (VDET) [8]. The tracking subdetectors are immersed in a uniform, axial 1.5 T magnetic field. The TPC is an Argon/Methane-filled cylinder extending radially from 0.3 to 1.8 m and providing up to 21 three-dimensional coordinates per track. The ITC is a cylindrical drift chamber with eight axial wire layers at radii from 16 to 26 cm. The VDET consists of two concentric cylinders of 300 μm thick silicon wafers at radii of 6.3 and 10.8 cm. The angular coverage of the inner layer is 0.84 in $|\cos\theta|$ and 0.69 for the outer layer. Each wafer provides measurements in $r\phi$ and rz views with an effective point resolution of 12 μm . The momentum resolution at 45 GeV/c when using all tracking subdetectors is $\Delta p/p^2 = 6 \times 10^{-4} (\text{GeV}/c)^{-1}$. The electromagnetic calorimeter (ECAL) and hadronic calorimeter (HCAL) are used to measure the energy of neutral particles and to identify leptons. The ECAL is a lead-wire chamber sandwich operating in proportional mode while the HCAL uses the iron return yoke as an absorber interspersed with tubes operated in limited streamer mode.

4 Event Selection and Acceptance

During 1991, 1992 and 1993, ALEPH accumulated 69 pb^{-1} of data. A total of 1.55×10^6 hadronic Z decays are obtained using a hadronic event selection based on charged tracks [9]. The background contamination of two-photon and $Z \rightarrow \tau^+\tau^-$ processes is estimated to be 0.3% and 0.2% respectively. Due to their low tagging efficiency and largely symmetric nature, they are safely neglected.

The average beamspot position is determined every 75 events and used to determine the event-by-event interaction point. This is done by projecting tracks onto the plane perpendicular to the jets (selected with the JADE algorithm [10] with a y_{cut} of 0.02) to which they belong. Combining this projection with the beamspot position, fixes the interaction point to a precision

Purity	Value
\mathcal{P}_u	1.88 (± 0.33) %
$\mathcal{P}_d, \mathcal{P}_s$	2.41 (± 0.43) %
\mathcal{P}_c	14.36 (± 0.79) %
\mathcal{P}_b	78.94 (± 1.45) %

Table 1: *Sample flavour composition at the nominal lifetime tag cut of 0.005.*

of $50 \times 10 \times 60 \mu\text{m}^3$ in horizontal, vertical and beam directions respectively. Track impact parameters are calculated in events with at least one track having VDET hits and a minimum of 2 jets with momenta above 10 GeV, lying further than 5.7 degrees from the beam.

Measurements of rates of single and double hemisphere tags are used with Monte Carlo estimates of correlations and background efficiencies to calculate the probability to tag a b quark hemisphere, ε_b^h . Events are selected if at least one hemisphere satisfies the lifetime tag cut. The cut is chosen to optimise the measurement sensitivity. The probability to tag an event of flavour f is :

$$\varepsilon_f^e = 2\varepsilon_f^h (1 - \rho_f \varepsilon_f^h) + \rho_f (\varepsilon_f^h)^2$$

where $\rho_f = \lambda_f(1/\varepsilon_f^h - 1) + 1$, and λ_f is the correlation between hemispheres. The flavour composition calculation makes use of the Z decay partial widths, $R_f = \Gamma_{f\bar{f}}/\Gamma_{had}$. This is given in Table 1 for the nominal lifetime tag cut of 0.005. In the case of the b quark, the measured R_b from [5] is used and Standard Model values are assumed for lighter flavours.

The thrust axis is determined using charged and neutral particle information. Its angle relative to the beam, θ_T , is used to define the original $f\bar{f}$ direction. The tagging efficiency is shown as a function of $\cos\theta_T$ in Figure 2. Expected tagging efficiencies of individual flavours are also shown assuming the flavour composition of Table 1. At angles greater than $\cos\theta_T = 0.8$ the tagging efficiency is limited by VDET geometry. In the same region, the efficiencies of b and c quarks are changing at different rates. This leads to a variation of the flavour composition close to the edge of acceptance. An acceptance of $0 < |\cos\theta_T| < 0.8$ only slightly reduces the b acceptance factor whilst minimising uncertainties from tagging in the low angle region. This selection leaves a total of 219,931 events at a lifetime tag cut of 0.005, with an estimated b selection efficiency of $63.91(\pm 0.98)\%$.

The acceptance factors, defined in (3), are calculated using Monte Carlo simulation where the total efficiency is constrained by data. Remaining differences are used to determine systematic errors. The acceptance factors are 0.821 for (u, d, s) quarks, 0.801 for c and 0.841 for b quarks.

5 Charge Asymmetry Measurements

Hemisphere charges are calculated using (1). Charged tracks with their point of closest approach to the beam within a cylinder of radius 2 cm and length 10 cm, more than 4 TPC hits, a polar angle ($\cos\theta$) less than 0.95 and a p_T relative to the beam of greater than 200 MeV/c are used. $\langle Q_{FB} \rangle$ and $\langle Q \rangle$ are measured for κ values between 0.3 and 2 with lifetime tag cuts corresponding to a range of \mathcal{P}_b from 73 to 95%. The measurement sensitivity is optimised using :

$$\mathcal{S} = \frac{\langle Q_{FB}^{exp} \rangle \sqrt{N}}{\sigma_{FB}}$$

where N and σ_{FB} are the observed number of tagged events and charge flow width respectively. $\langle Q_{FB}^{exp} \rangle$ is the expected charge asymmetry for a given $\sin^2\theta_W^{eff}$, κ and flavour composition.

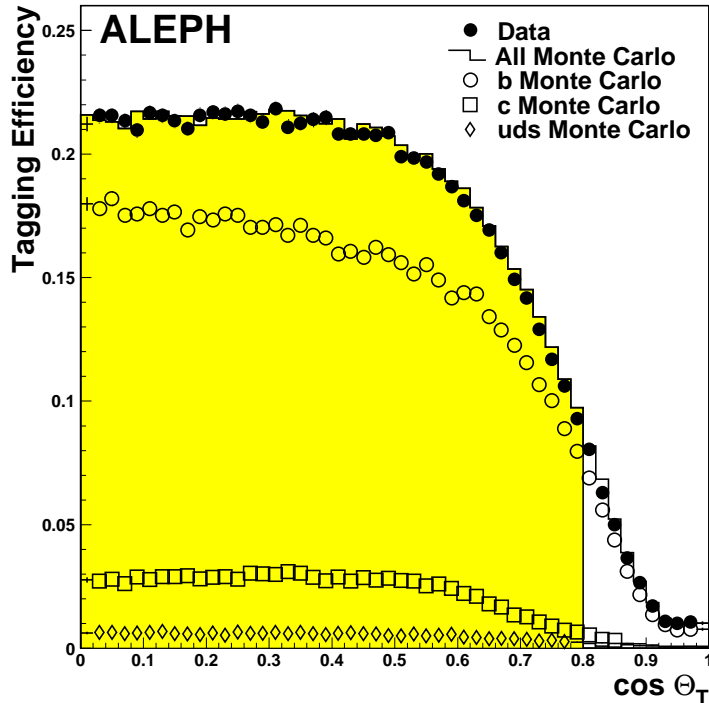


Figure 2: *Event tagging efficiencies in data and Monte Carlo simulation as a function of $\cos \theta_T$. The shaded region indicates the measurement acceptance.*

Optimum sensitivity is found at $\kappa=0.7$ and a lifetime tag cut corresponding to a b purity of 79%. This is independent of $\sin^2 \theta_W^{eff}$. The mean charge flow and the total charge at this nominal working point are measured to be :

$$\begin{aligned} \langle Q_{FB} \rangle &= -0.01042 \quad (\pm 0.00088 \text{ stat.}) \\ \langle Q \rangle &= +0.00514 \quad (\pm 0.00077 \text{ stat.}) \end{aligned} \quad (4)$$

The interaction of particles in the material prior to the tracking subdetectors leads to a non-zero total charge due to the charge dependence of nuclear cross-sections. The consequences of this are included as a systematic error.

The experimental systematic errors on $\langle Q_{FB} \rangle$ arise from sources which are both forward-backward and charge asymmetric. These are either due to an incorrect tracking response or an forward-backward imbalance of detector material. Tracking response is studied by comparing the mean momenta of particles with the beam energy in collinear $Z \rightarrow \mu^+ \mu^-$ decays. Differences between positive and negative tracks are typically less than 1.5% and therefore the effect on $\langle Q_{FB} \rangle$ is small. The sensitivity of $\langle Q_{FB} \rangle$ to the track selection is studied by excluding tracks close to cuts and also those identified as having pattern recognition problems leading to momenta greater than 50 GeV/c. The asymmetry in the material distribution of ALEPH are monitored using photon conversions and is determined to be $1.8 \pm 1.6\%$. It is combined with the total charge, $\langle Q \rangle$, to give a systematic uncertainty on $\langle Q_{FB} \rangle$. A summary of experimental systematic errors is given in Table 2.

6 Calibration of the Charge Separations

It is clear from relation (3) that a precise δ_b measurement is important for the extraction of A_{FB}^b . Uncertainties from lighter quark flavours are suppressed by their low tagging efficiency. Hence

<i>Systematic Error Source</i>	$\Delta\langle Q_{FB} \rangle (\times 10^{-4})$
<i>Tracking Momentum imbalance</i>	+0.01 (± 0.01)
<i>Effect of Cut on closest approach to beam in xy</i>	+0.01 (± 0.26)
<i>Effect of Cut on closest approach to beam in z</i>	-0.06 (± 0.09)
<i>Effect of Cut on minimum angle to the beam</i>	+0.11 (± 0.43)
<i>Effect of Cut on number of track hits</i>	-1.22 (± 0.69)
<i>Effect of tracks with $p > 50$ GeV/c</i>	+0.47 (± 0.52)
<i>Material asymmetry</i>	+0.93 (± 0.84)
<i>Total Systematic Uncertainty</i>	1.61×10^{-4}

Table 2: *Summary of experimental systematic errors.*

δ_b is extracted from data whilst δ_{uds} are estimated from Monte Carlo simulation. A modified version of the JETSET [11, 3] model is used for the latter.

Using relation (2) to extract δ_b requires knowledge of $\bar{\delta}_b$, ie. a measurement of $\bar{\delta}$ in a pure sample of b events. In practice, this is difficult to achieve with the required statistical precision. A fitting procedure is used instead to extrapolate $\bar{\delta}$ measurements at different b purities to $\mathcal{P}_b = 100\%$. The measurements are shown in Figure 3 where the $\bar{\delta}$ values are corrected for a kinematical bias induced by successive lifetime tag cuts. The bias is observed in data when comparing tagged and untagged hemispheres of singly tagged events. Events with many high momentum charged tracks are more likely to have significant impact parameters and well defined hemisphere charges. In general, tagged hemispheres have an 8 to 12% better charge resolution than untagged hemispheres. Corrections of less than 7% are applied to $\bar{\delta}$ with a relative uncertainty of 30% from differences between data and Monte Carlo.

The dependence of $\bar{\delta}$ on the flavour composition may be understood by considering :

$$\bar{\delta} = \sqrt{\sum_{f=u,d,\dots}^b \mathcal{P}_f \bar{\delta}_f^2}$$

It is expected that δ_u is the largest charge separation and so $\bar{\delta}$ is expected to decrease with harder lifetime tag cuts. With stringent lifetime selections, effectively only b quarks remain with a small c contamination. The opposite behaviour of δ_b and δ_c with κ then becomes important. At low κ , $|\delta_c|$ is greater than $|\delta_b|$ with $|\delta_b|$ becoming larger thereafter. This slightly increases $\bar{\delta}$ as $\mathcal{P}_b \rightarrow 100\%$ for κ values above 0.7. A cubic polynomial is used to describe the full behaviour. The fitted curves are shown in Figure 3.

To calculate δ_b from extrapolated values of $\bar{\delta}_b$, the correlation between measurement errors, $\langle \mathcal{R}_f \mathcal{R}_{\bar{f}} \rangle$ in equation (2), is derived from Monte Carlo simulation. Its dependence on fragmentation is tested by varying model parameters. No significant dependence is observed and a conservative systematic uncertainty is ascribed to each parameter variation. The value of $\langle \mathcal{R}_f \mathcal{R}_{\bar{f}} \rangle$ at a κ of 0.7 is 0.0066 ± 0.0004 (*stat.*) ± 0.0011 (*syst.*). The $\langle Q_{FB} \rangle^2$ and $\langle Q \rangle^2$ corrections in equation (2) are measured in a 95% pure sample of data although their contribution to δ_b is small. The extracted value of δ_b at a κ of 0.7 is

$$\begin{aligned} \delta_b = & -0.1706 \pm 0.0023 \text{ (data statistics)} \\ & \pm 0.0038 \text{ (Monte Carlo statistics)} \\ & \pm 0.0019 \text{ (lifetime tag bias systematics)} \\ & \pm 0.0027 \text{ (measurement error correlation systematics)} \end{aligned}$$

Charge separations for lighter quark flavours ($\delta_{u,d,s,c}$) are also estimated from Monte Carlo

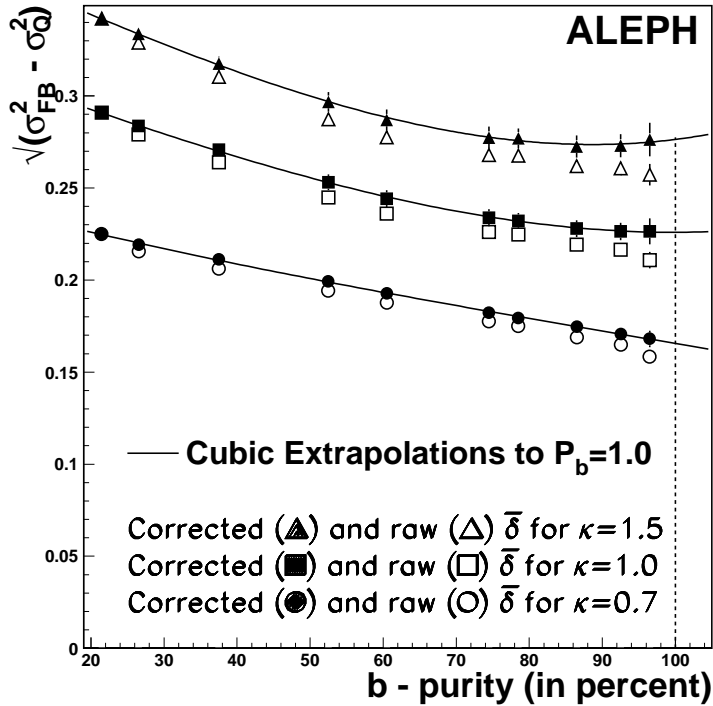


Figure 3: Measured and lifetime tag corrected values of $\bar{\delta} = \sqrt{(\sigma_{FB}^2 - \sigma_Q^2)}$ as a function of the b purity.

Separation	δ_f	$\Delta\delta_f (stat.)$	$\Delta\delta_f (syst.)$
δ_u	+0.306	± 0.007	± 0.022
δ_d	-0.153	± 0.006	± 0.022
δ_s	-0.203	± 0.006	± 0.019
δ_c	+0.170	± 0.001	± 0.021
δ_b	-0.169	± 0.002	± 0.005

Table 3: Summary of charge separations used at the nominal κ and flavour composition.

simulation. Model parameter variations are used to assign systematic uncertainties and are typically between 10 and 20%.

A final correction is applied for the small dependence of separations on the lifetime tag cut at which $\langle Q_{FB} \rangle$ is measured. This remains below 1% for δ_b at the nominal κ and lifetime tag cut. The separations and errors used to extract A_{FB}^b are summarised in Table 3.

7 Results

In order to treat the background contributions from lighter quark flavours in equation (3) consistently, A_{FB}^b is measured by extracting the value of $\sin^2\theta_W^{eff}$ which best fits the data. Electroweak corrections are applied [1] to pole asymmetries for initial and final state QED radiation, $\gamma - Z$ interference and photon exchange¹. No correction for QCD radiation is applied beyond that which enters through the measurement of δ_b . The measured asymmetry is slightly diluted by the thrust axis resolution. This is treated as a systematic error and estimated to be

¹A Higgs mass of $300 GeV/c^2$ is assumed throughout.

Source of Systematic Error	ΔA_{FB}^{bb}	$\Delta \sin^2\theta_W^{eff}$
Systematic Error on δ_b	0.0032	0.00060
Stat. and Syst. Error on Tag Purity	0.0019	0.00035
Experimental Systematics on $\langle Q_{FB}^{btag} \rangle$	0.0017	0.00033
Systematic Error on $\delta_{u,d,s,c}$	0.0016	0.00029
Statistical Error on δ_b	0.0014	0.00027
Systematic from thrust axis resolution	0.0004	0.00007
Statistical Error on the Acceptance	0.0002	0.00005
Systematic Error on the Acceptance	0.0002	0.00005
Statistical Error on $\delta_{u,d,s,c}$	0.0002	0.00003
Total Systematic Error	0.0046	0.00087

Table 4: Summary of systematic errors on A_{FB}^{bb} and $\sin^2\theta_W^{eff}$ for a κ of 0.7 with a lifetime tag cut of 0.005.

-0.07% from Monte Carlo. LEP ran at 9 different energies during 1991, 1992 and 1993. Taking into account the energy distribution of data gives a correction of 0.08% to A_{FB}^b by moving from the average energy to 91.187 GeV. Fitting the observed charge asymmetry in the sample yields an effective electroweak mixing angle of :

$$\sin^2\theta_W^{eff} = 0.2315 \pm 0.0016 (stat.) \pm 0.0009 (syst.)$$

At the Z peak, this corresponds to a forward-backward b asymmetry of :

$$A_{FB}^b = 0.0992 \pm 0.0084 (stat.) \pm 0.0047 (syst.)$$

Systematic error contributions are summarised in Table 4. The dominant systematic error arises from the δ_b measurement, and specifically from the measurement error correlation and kinematical bias introduced by the lifetime tag. The stability of results with respect to κ and flavour composition is shown in Figure 4. No significant discrepancy is observed when correlations between statistical and systematic errors are taken into account. Measured values of A_{FB}^b versus \sqrt{s} are compared with expectations in Figure 5. The expected gradient is independent of $\sin^2\theta_W^{eff}$ and in good agreement with data.

8 Conclusions

A significant charge asymmetry is observed in heavy flavour Z decays selected using track impact parameters. In a 79% pure sample of $b\bar{b}$ decays the mean charge flow is :

$$\langle Q_{FB} \rangle = -0.01042 \pm 0.00088 (stat.) \pm 0.00016 (syst.)$$

In the Standard Model, all quark asymmetries are determined by an effective electroweak mixing angle. Using a measurement of the reconstructed b quark charge, this is determined to be :

$$\sin^2\theta_W^{eff} = 0.2315 \pm 0.0016 (stat.) \pm 0.0009 (syst.)$$

and is interpreted as being due to a forward-backward b asymmetry of :

$$A_{FB}^b = 0.0992 \pm 0.0084 (stat.) \pm 0.0046 (syst.)$$

This asymmetry can be combined with the previous ALEPH measurement of $A_{FB}^b = 0.087 \pm 0.014 \pm 0.002$ [3] based on semileptonic decays. Event samples and systematic errors are almost entirely independent and the combined value of A_{FB}^b is 0.0953 ± 0.0080 .

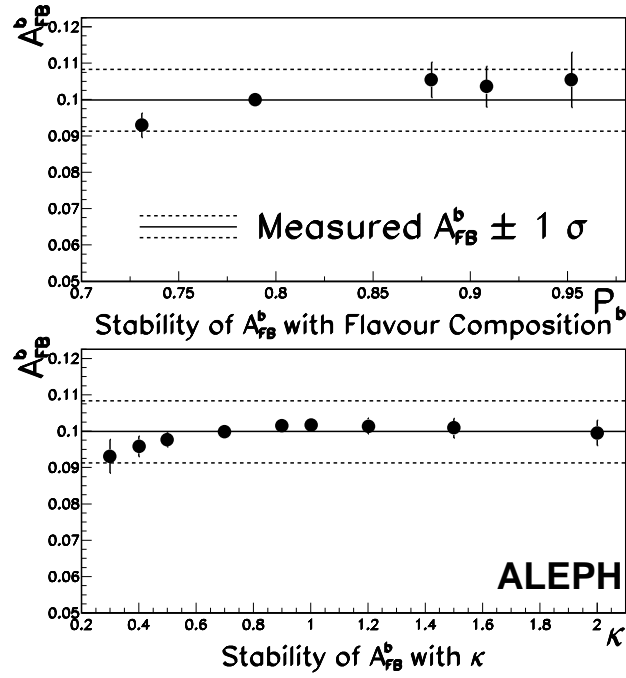


Figure 4: A_{FB}^b for different flavour compositions and κ values. Uncorrelated statistical and systematic errors relative to the measured value are shown.

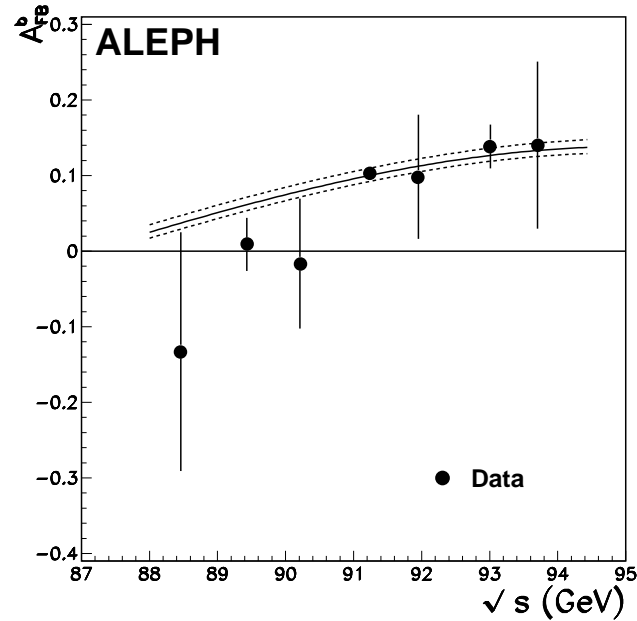


Figure 5: Variation of A_{FB}^b with centre-of-mass energy. Statistical errors only are shown. The theoretical curves shown correspond to a $\sin^2\theta_W^{eff}$ of 0.2315 ± 0.0018 .

9 Acknowledgements

We wish to thank our colleagues from the accelerator divisions for the successful operation of LEP. We are indebted to the engineers and technicians of the ALEPH collaborating institutes for their contribution to the excellent performance of the detector. Those of us from non-member countries thank CERN for its hospitality.

References

- [1] D. Bardin et al, CERN TH **6443-92**, (1992).
- [2] B. Lampe, MPI Preprint, **MPI-Ph/93-74**, (1993).
- [3] The ALEPH Collaboration, D. Decamp et al, CERN Preprint, **CERN-PPE/94-017**, (Accepted by Z. Phys. C.), (1994).
- [4] The DELPHI Collaboration, P. Abreu et al, *Physics Letters*, **B 276** 536, (1992).
The L3 Collaboration, D. Adriani et al, *Physics Letters*, **B 292** 454, (1992).
The OPAL Collaboration, P. D. Acton et al, CERN Preprint, **CERN-PPE/93-078**, (Submitted to Z. Phys. C.), (1993).
- [5] The ALEPH Collaboration, D. Decamp et al, *Physics Letters*, **B 313** 535, (1993).
- [6] The ALEPH Collaboration, D. Decamp et al, *Physics Letters*, **B 259** 377, (1991).
- [7] The ALEPH Collaboration, D. Decamp et al, *Nucl. Inst. & Methods* **A294** 121, (1990).
- [8] The ALEPH Collaboration, Conference record of the 1991 IEEE Nuclear Science Symposium, Sante Fe, New Mexico. **Volume 1** 444, (1991).
- [9] The ALEPH Collaboration, D. Decamp et al, *Physics Letters*, **B 231** 519, (1989).
- [10] The JADE Collaboration, C. Kleinwort et al, *Z. Phys. C.* **42** p7, (1989).
- [11] T. Sjöstrand, *Computer Physics Commun.* **39** 347, (1986).
T. Sjöstrand and M. Bengtsson, *Computer Physics Commun.* **43** 367, (1987).